The many faces of synapsid cranial allometry

Authors: Krone, Isaac W., Kammerer, Christian F., and Angielczyk, Kenneth D.

PALEOBIOLOGY
A PUBLICATION OF THE
Paleontological
SOCIETY

Article

The many faces of synapsid cranial allometry

Isaac W. Krone ⓘ*, Christian F. Kammerer, and Kenneth D. Angielczyk*

Abstract.—Previous studies of cranial shape have established a consistent interspecific allometric pattern relating the relative lengths of the face and braincase regions of the skull within multiple families of mammals. In this interspecific allometry, the facial region of the skull is proportionally longer than the braincase in larger species. The regularity and broad taxonomic occurrence of this allometric pattern suggests that it may have an origin near the base of crown Mammalia, or even deeper in the synapsid or amniote forerunners of mammals. To investigate the possible origins of this allometric pattern, we used geometric morphometric techniques to analyze cranial shape in 194 species of nonmammalian synapsids, which constitute a set of successive outgroups to Mammalia. We recovered a much greater diversity of allometric patterns within nonmammalian synapsids than has been observed in mammals, including several instances similar to the mammalian pattern. However, we found no evidence of the mammalian pattern within Therocephalia and nonmammalian Cynodontia, the synapsids most closely related to mammals. This suggests that the mammalian allometric pattern arose somewhere within Mammaliaformes, rather than within nonmammalian synapsids. Further investigation using an ontogenetic series of the anomodont *Diictodon feliceps* shows that the pattern of interspecific allometry within anomodonts parallels the ontogenetic trajectory of *Diictodon*. This indicates that in at least some synapsids, allometric patterns associated with ontogeny may provide a "path of least resistance" for interspecific variation, a mechanism that we suggest produces the interspecific allometric pattern observed in mammals.

Isaac W. Krone.* University of Chicago, Chicago, Illinois 60637, U.S.A. E-mail: isaacwkrone@gmail.com. *Present address: Museum of Vertebrate Zoology, University of California, Berkeley, California 94720-3161, U.S.A.

Christian F. Kammerer. North Carolina Museum of Natural Sciences, Raleigh, North Carolina 27601-1029, U.S.A. E-mail: christian.kammerer@naturalsciences.org

Kenneth D. Angielczyk. Integrative Research Center, Field Museum of Natural History, 1400 South Lake Shore Drive, Chicago, Illinois 60605-2827, U.S.A. E-mail: kangielczyk@fieldmuseum.org

Introduction

The cranium is a highly complex structure that has evolved myriad forms associated with many different ecologies throughout the tetrapod radiation. Despite this fact, tetrapod crania all exhibit a shared basic architecture— a braincase and associated sensory capsules and a facial skeleton associated with the jaws (Emerson and Bramble 1993)—facilitating comparisons across the group. Many tetrapod clades also have an extensive fossil record including well-preserved crania. These clades provide excellent systems in which to study both small- and large-scale patterns in shape evolution over time. Recent large-scale analyses of tetrapod crania have used geometric morphometric techniques to address questions of disparity and allometry within a variety of major tetrapod groups (e.g., Stayton 2005; Goswami 2006; Goswami and Polly 2010; Angielczyk and Ruta 2012; Bhullar et al. 2012; Brusatte et al. 2012; Foth and Rauhut 2013; Zelditch and Calamari 2016), including those with idiosyncratic or highly derived cranial structures (Claude et al. 2004; Sherratt et al. 2014; Churchill et al. 2018). However, little work has been done to synthesize the results of these analyses or to look for pan-tetrapod morphological patterns.

One such pan-tetrapod pattern has been suggested, albeit obliquely, by analyses of cranial allometry in crown mammals. Within otherwise morphologically conservative mammalian families, there exists a widespread pattern of interspecific allometry in which larger animals have proportionally longer faces (Radinsky 1985; Cardini and Polly 2013; Cardini et al. 2015; Cardini 2019). Studies

using geometric morphometric techniques have suggested that this trend is a salient and widespread pattern of cranial allometry within Mammalia, characterizing groups as disparate as antelopes (Antilopinae and Cephalopinae), fruit bats (Pteropodidae), African mongooses (Herpestidae), African tree squirrels (Sciuridae) (Cardini and Polly 2013), cats (Felidae) (Tamagnini et al. 2017), and kangaroos (Macropodidae) (Cardini et al. 2015; but see Mitchell et al. 2018). Cardini et al. (2015) referred to this pattern of snout length allometry within closely related and morphologically conservative groups as the "cranial rule of evolutionary allometry," or CREA, and suggested that it may be as widespread as Bergmann's rule and Allen's rule, extending to nearly all mammals.

If it is indeed so ubiquitous, the CREA pattern demands explanation. Cardini and Polly (2013) suggested that the pattern may be driven by disparity in allometric scaling between the body, the jaw, and the brain. Because brain size scales with a ¾ exponent relative to body mass (Martin et al. 2005), and jaw length (under isometry) should scale with a ⅓ exponent relative to body mass, the relative length of the braincase should scale at a lower rate than the jaw. This produces a pattern of cranial allometry in which larger animals have relatively longer faces, because the snout must grow in line with the jaw to allow effective feeding. Due to the shared architecture of tetrapod crania and the difference in growth rate between the braincase and the jaw, this explanation, if valid, predicts an extension of the CREA pattern to all tetrapods.

Cardini and Polly (2013) also noted the interrelationship between ontogenetic allometry in mammals and the observed pattern of interspecific allometry with respect to the relative size of the snout. Juvenile mammals generally display a higher degree of brachycephaly compared with adults of the same species, creating an ontogenetic pattern that mirrors CREA. They posited that this allometric relationship constrains the degree to which heterochronic shifts in the rate of development of the facial region can operate to change adult snout length in mammals. They also suggested that this link between size and shape allows shape adaptation to proceed through changes in body size.

Outside of mammals, fewer studies have explicitly focused on large-scale analyses of allometry within tetrapod crania. Angielczyk and Ruta (2012) found a pattern similar to CREA within Permo-Carboniferous temnospondyl amphibians. Smaller temnospondyls tended to have short, broad snouts, whereas larger temnospondyls had proportionally longer snouts. In addition, Bright et al. (2016) and Linde-Medina (2016) recovered CREA-like patterns in raptors and Galliformes, respectively, using geometric morphometric techniques, though Linde-Medina found a traditional morphometric approach does not recover a CREA-like pattern and suggested that the use of centroid size as a predictor variable may be problematic.

Because temnospondyls, mammals, and birds represent each of the three great lineages of crown tetrapods that diverged in the Carboniferous (Benton et al. 2015), it is possible that a CREA-like allometric pattern is common to all tetrapods, in line with Cardini and Polly's (2013) scaling hypothesis. If the similar allometric patterns in temnospondyls, birds, and mammals reflect an ancestral tetrapod pattern, we would expect a CREA-like pattern to characterize nonmammalian synapsids, the now-extinct members of the mammalian stem lineage. Alternatively, if the CREA pattern is not an ancestral tetrapod trait, we predict that other patterns of cranial allometry would be present in nonmammalian synapsids, although some synapsids might have evolved a similar allometric relationship independently. The evolution of synapsid skull characters is well-studied (e.g., Kemp 1982, 2005; Hopson 1991; Sidor and Hopson 1998; Sidor 2001; Esteve-Altava et al., 2013; Benoit et al. 2016; Angielczyk and Kammerer 2018), and the overall trend toward a more mammal-like skull within therapsids offers the possibility of pinpointing when this pattern of interspecific allometry evolved.

For this study, we assembled a photographic library of lateral-view images of nonmammalian synapsid crania for use in geometric morphometric analyses. Our sample includes all major groups of "pelycosaur"-grade synapsids (Caseasauria [Eothyrididae + Caseidae], Varanopidae, Ophiacodontidae, Edaphosauridae, Sphenacodontidae) and therapsids (Biarmosuchia, Dinocephalia,

Anomodontia, Gorgonopsia, Therocephalia, non-mammalian Cynodontia) and represents the majority of well-preserved synapsid whole-cranium fossils. We used this data set to test for a CREA-like pattern in "pelycosaurs" as well as in each major therapsid subclade. To investigate similarity between interspecific and ontogenetic allometry in nonmammalian synapsids, we also analyzed a set of 39 specimens of the anomodont *Diictodon feliceps* and compared their ontogenetic trajectory with the interspecific allometric pattern recovered across Anomodontia. We made a similar comparison between an ontogenetic series of 26 specimens of the therocephalian *Theriognathus microps* and the interspecific allometric patterns in Therocephalia as a whole.

Materials and Methods

Phylogenetic Framework and Timescale Data

Our analyses focus on seven synapsid subgroups. Five of these groups are therapsid clades: Biarmosuchia, Dinocephalia, Anomodontia, Gorgonopsia, and Therocephalia. The other two groups, "pelycosaurs" and nonmammalian cynodonts, constitute evolutionary grades. Cynodontia contains Mammalia, rendering our sample of cynodonts paraphyletic. "Pelycosaurs" consist of a grade at the base of Synapsida containing several ecologically and anatomically distinct clades that serve as successive outgroups to Therapsida. Because of low sample sizes in the component family-level "pelycosaur" clades, we analyzed "pelycosaurs" as a group.

We used published phylogenies for "pelycosaurs" (Brocklehurst et al. 2016), Biarmosuchia (Kruger et al. 2015), Dinocephalia (Kammerer 2011), Anomodontia (Angielczyk and Kammerer 2017), Gorgonopsia (Kammerer and Masyutin 2018), Therocephalia (Sigurdsen et al. 2012), and Cynodontia (Ruta et al. 2013) to construct topologies for time-scaled trees for each group. Any taxa or specimens not included in these trees were grafted on based on current taxonomy. Using these clade-specific trees, we then constructed a supertree following the prevailing hypothesis for branching order of the major synapsid clades (Sidor and Hopson 1998; Angielczyk and Kammerer 2018). Branch lengths for the trees were calculated using the equal branch length method

(Brusatte et al. 2008) implemented in the R package strap (Bell and Lloyd 2015), with species temporal occurrence data taken from the Paleobiology Database (paleobiodb.org) and other literature sources. First and last occurrence dates were binned by stratigraphic stage, and root lengths were added based on first occurrence data for the outgroup to each tree according to the branching order of our synapsid supertree. Our supertree can be found in the Supplementary Material for this paper.

Thirteen skulls could not be assigned to currently recognized species. In 10 cases, we assigned the specimens to genera (MMK 513 and NMQR 3512: *Pristerognathus*; CGS CM86-600, SAM-PK-708, SAM-PK-775, SAM-PK-6623, SAM-PK-7850, SAM-PK-K10703, SAM-PK-K11 177: *Emydops*; USNM 487098: *Ophiacodon*), and in two cases, we assigned them to unnamed species (NHCC LB277: *Abdalodon* sp.; NHCC LB178: *Lycaenops* sp.) that were then used as terminal taxa in our trees and analyses. We treated these taxa identically to species-level taxa in our analyses.

Photography

We assembled a database of 910 photographs representing 461 nonmammalian synapsid crania. The majority of the specimens used in this study were photographed at their host institutions using a Sony Cyber-shot 7.2 megapixel camera. Additionally, a large number of dicynodonts and some other specimens were photographed in their host institutions using a Canon EOS Rebel DSLR. All photos included a scale bar of at least 1 cm. Specimens were photographed in lateral view and set against a contrasting background when possible. Twenty-one specimens in the initial data set were discarded, because they were either considered too badly distorted or incomplete to use or were represented by inadequate photographs. We considered photographs to be inadequate if they lacked a scale bar or were angled such that the shape of the skull was badly distorted due to perspective or parallax issues.

Digitization

Our final data set contains data from 440 crania, representing 194 taxa of nonmammalian synapsids. Information on the specimens

and species included can be found in Supplementary Table 1.

One of us (I.W.K.) digitized 12 two-dimensional landmarks on the lateral surface of every specimen using TPSDig2 (v. 2.26) (Rohlf 2016), digitizing both right and left lateral views of the skull when adequate images of both sides were available. Images of the right side of the skull were mirrored digitally so that all landmark data correspond to left lateral views. Many specimens were only able to be digitized on one side due to poor preservation. For the final analyses, only landmark configurations from the best-preserved side of the skull for each specimen were used. We calibrated the absolute size of the landmark data in TPSDig2 using a 1- to 5-cm-long reference length from the scale bars included in the photos. To assess the repeatability of landmark placement, I.W.K. digitized 10 *D. feliceps* specimens, repeating digitization of the full set 10 times, and compared variance within resampling trials of each specimen and between consensus data sets of all specimens. Average variance within specimens was 24× less than variance among the 10 specimens (σ^2 = 0.000436 vs. σ^2 = 0.0107).

Landmark Configuration

The extreme disparity in both anatomy and preservation quality of the specimens analyzed limited the number of homologous landmarks that could be consistently placed in the set of photographs. The majority of landmarks rely on geometric evidence (type 2) or partially rely on other landmarks to determine their position (type 3), rather than relying on sutures or other structural features (type 1) (see Bookstein [1991] for discussion of landmark types). In some cases (e.g., landmark 4), differences in anatomy and preservation meant that morphological proxies were used for landmark placements. The 12 landmarks chosen characterize the snout, orbit, temporal region, and cranial vault (Fig. 1, Table 1). Five landmarks (landmarks 1–5) make up the snout/face region and seven (landmarks 6–12) make up the braincase region. Though landmarks 6–12 do not all capture the braincase per se, they provide a proxy for the size and shape of the braincase region and allow some comparability to previous studies uncovering the CREA pattern.
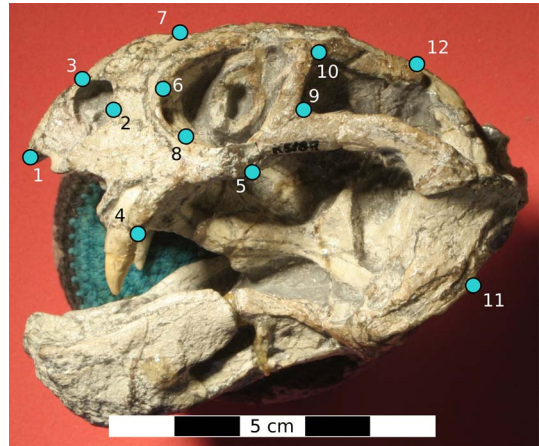

FIGURE 1. Landmark configuration. *Diictodon feliceps* specimen (SAM-PK-K5189) with landmarks placed according to the configuration found in Table 1.

Landmarks were not placed on the occipital, basicranial, and anterior palatal regions for several reasons. First, the morphological disparity in some of these areas is so great that

TABLE 1. Landmark positions. *These teeth are absent/not preserved in many taxa; however, this is just anterior to the point of greatest curvature on most maxillae. [†]In cynodont taxa lacking a postorbital bar, this was marked as the tip of the postorbital process of the frontal.

Number	Region	Type	Description
1	Face	2	Anteroventral tip of premaxilla
2	Face	2	Posterior margin of naris
3	Face	3	Dorsal margin of skull above anterior margin of naris
4	Face	1	Intersection of posterior margin of posterior canine/enlarged maxillary caniniform tooth and ventral margin of the maxilla*
5	Face	1	Posterior tip of maxilla
6	Braincase	2	Anterior margin of orbit
7	Braincase	3	Dorsal surface of skull above landmark 6
8	Braincase	2	Midpoint on ventral margin of orbit
9	Braincase	1	Anteroventral corner of temporal fenestra
10	Braincase	1	Anterodorsal corner of temporal fenestra[†]
11	Braincase	2	Posteroventral margin of squamosal
12	Braincase	3	Midpoint on skull vault (behind parietal foramen, if visible)

establishing homology is quite difficult, particularly near the jaw articulation, a region of extreme morphological transformation within early synapsids. Second, a lack of clear sutures and a great diversity of component bones in these areas make landmarks difficult to place with any certainty. Third, many taxa either lack certain features that were considered as landmark candidates (e.g., dicynodonts lack a transverse process of the pterygoid, which establishes the anterior extreme of the braincase) or have features that obscure parts of their anatomy (e.g., in many synapsids, the squamosal extends posteriorly beyond the plane of the occiput, making landmarks in the occipital region impossible to assess from a lateral view; furthermore, in many specimens, the lower jaw is preserved in articulation with the skull, obscuring the palate and basicranium). Fourth, the basicranial and anterior palatal regions tend to be the most poorly preserved and prepared regions in synapsid skull fossils. Because of these difficulties, our conclusions may be less robust than those of an analysis in which many clearly homologous landmarks could be reliably located. Nevertheless, our landmark configuration does provide adequate information to assess the relative sizes of the preorbital and postorbital regions of the skull.

Analyses

All of the analyses in this study were performed using the R package Geomorph 3.0.1 (Adams et al. 2016). For each synapsid subgroup, we constructed a data set consisting of one landmark configuration for each specimen. We then performed missing landmark estimation using thin-plate spline interpolation (Gunz et al. 2009). This step was necessary due to specimens in which some landmarks were unable to be placed because of poor preservation of the fossil. Any specimen for which five or more landmarks could not be confidently placed was removed from the sample. Percentages of missing landmarks in the data are as follows: "pelycosaurs," 7.00%; Biarmosuchia, 5.83%; Dinocephalia, 4.57%; Anomodontia, 6.74%; Gorgonopsia, 7.41%; Therocephalia, 6.76%; nonmammalian cynodonts, 7.43%; *Diictodon*, 4.50%; *Theriognathus*, 5.02%.

After completing missing landmark estimation, we grouped specimens according to taxon (tip taxa in our phylogeny) and performed a generalized Procrustes analysis on the landmark data from the specimens, which generated consensus (mean) landmark configurations (with associated mean centroid size) for each tip taxon represented by more than one specimen. We then concatenated data for these mean shapes together with shapes for species represented by only one specimen to create final data sets containing one landmark configuration for each tip taxon.

For Anomodontia, we performed a simple linear regression using the *lm() function* (R Core Team 2017) to determine whether size changed over time within the clade, regressing log centroid size against first occurrence time for each species. We also tested for phylogenetic signal in log centroid size using the *phylosig()* function in phytools (Revell 2012), using the Wilks's lambda method.

Analysis of Allometry

In all tests of allometry, we used log-transformed centroid size as a variable to predict changes in shape. Though it has been suggested that this approach may bias studies toward recovery of the CREA pattern (Linde-Medina 2016), we use centroid size here in accordance with Tamagnini et al. (2017) and Cardini (2019), who find it to correspond well with other methods of measurement. This also allows for more direct comparability with previous mammalian studies (Cardini and Polly 2013; Cardini et al. 2015; Tamagnini et al. 2017; Mitchell et al. 2018; Cardini 2019). To investigate whether nonmammalian synapsid groups share a common allometric pattern, we performed a phylogenetic generalized least-squares (PGLS) regression with a Brownian motion model of evolution using the geomorph function *procD.pgls* on a data set including all species in our study and using our concatenated supertree. We tested three models for the relationship between size and shape in nonmammalian synapsids: (1) cranial shape is explained by size (shape ~ size), (2) cranial shape is explained by size and group membership (shape ~ size + group), and (3) cranial shape is explained by size and group

membership, with different groups having different allometric trajectories (shape ~ size * group). Because a corrected Akaike information criterion framework does not exist for these procD analyses, we compared the models based on their significance levels and R^2 values, selecting as favored the model with highest significance and best fit. To visualize differences in allometric trajectory, we plotted the PC 1 of predicted shapes from the PGLS regression versus log-transformed centroid size (Adams and Nistri 2010).

We also analyzed shape change in each synapsid subgroup independently to assess allometric patterns on a taxonomic scale similar to that of the mammalian family-level clades used by Cardini and Polly (2013) and Cardini et al. (2015). For each subgroup, we performed a Procrustes distance–based generalized Procrustes analysis to remove the effects of size and rotation in the data set. We then performed a principal component analysis of the resulting Procrustes-aligned data to assess the effects of taphonomic distortion and size on major components of shape variation.

To assess and visualize covariation between size and shape, we performed a Procrustes ANOVA regression on each synapsid subgroup using the geomorph *procD.lm* function, with 1000 replicates to test for significance. We used PGLS regression to test whether the changes in shape recovered using the Procrustes ANOVA regression method were significant within a phylogenetic context. For each synapsid subgroup, these tests were performed both with shape (Procrustes distance) as the response variable and with PC 1–3 of morphospace as response variables to investigate how allometric patterns may influence major axes of shape variation. Here we report only phylogenetically corrected (PGLS) results, except in Anomodontia and Therocephalia, the groups in which we directly compared intraspecific allometry with ontogenetic allometry. In anomodonts, we found that the phylogenetically corrected regression did not recover an important pattern of allometry that was recovered using generalized least-squares (GLS) regression (see "Discussion"). In all tests, we used log-transformed centroid size as the predictor variable.

To assess similarity between ontogenetic and interspecific allometric trajectories in Anomodontia and Therocephalia, we combined data sets for ontogenetic series of *D. feliceps* and *T. microps* with the interspecific data sets for Anomodontia and Therocephalia, respectively. After performing Procrustes superimposition on these data sets, we regressed all shape components on log centroid size and performed a homogeneity of slopes test with 1000 replicates to determine whether the allometric trajectories in the selected species and their parent clades share a common slope, using the *procD.allometry* function in geomorph. In addition to the homogeneity of slopes test, we performed an angular comparison of vector directions (Zelditch et al. 2003) between recovered interspecific and ontogenetic allometric trajectories in these combined data sets using Geomorph's *procD.lm* function. We then generated 1000 alternative allometric trajectories for ontogenetic and interspecific shape data set by randomly reordering centroid size within the data set before recovering trajectories using *procD.lm* and compared the magnitude of observed angles between ontogenetic and interspecific allometric trajectories with the magnitude distributions of these alternative angles to obtain a *p*-value for the observed angles.

Results

Analyses of Allometry

All Nonmammalian Synapsids.—There is a significant but weak relationship between size and shape in our data set of all synapsid crania ($R^2 = 0.0197$, $p < 0.001$) (Table 2), but individual synapsid groups do not share allometric trajectories. Our best-fitting model is shape ~ size * group ($R^2 = 0.03174$, $p = 0.006$), in which shape is explained by size and group membership, with different groups having different trajectories (Fig. 2). Size does not correlate with PC 1 of synapsid morphospace, which is dominated by changes in relative snout length ($R^2 = 0.001$, $p = 0.642$), or PC 2, which is dominated by anterodorsal versus posterodorsal shearing ($R^2 = 0.015$, $p = 0.096$). PC 3 of synapsid morphospace involves changes in the relative size of the orbit and does correlate with size ($R^2 = 0.0974$, $p < 0.001$) (Supplementary Table S3).

TABLE 2.   Comparison of synapsid allometric trajectories. Results of phylogenetic generalized least-squares regression of log centroid size vs. all shape components using the formula shape ~ size * group membership. The p-values in italics are significant with a threshold of $p < 0.05$.

Explanatory variable	Sum of squares	Mean sum of squares	R squared	F-statistic	Z-statistic	p
Size	0.01119	0.0111909	0.0198	4.0083	3.1145	*0.0004*
Size + groups	0.01969	0.0032825	0.03485	1.1757	1.0064	0.1528
Size * group	0.03174	0.0052903	0.05616	1.8949	2.6066	*0.0064*

"Pelycosaurs".—The relationship between centroid size and skull shape in "pelycosaur"-grade synapsids is particularly strong ($R^2 = 0.278$, $p = 0.003$) (Table 3), with larger-skulled "pelycosaurs" having long snouts and a sphenacodontid- or ophiacodontid-like skull shape, whereas smaller-skulled "pelycosaurs" have shorter snouts and a caseid-like morphology (Figure 3). It is important to note, however, that centroid size here refers to the size of the head, not the overall size of the animal in question, and this relationship probably does not hold for the latter metric. Some "pelycosaurs," such as caseids, have very small heads relative to their large, robust bodies, whereas others, such as ophiacodontids, have proportionally much larger heads. This suggests a significant phylogenetic component to the size–shape relationship, yet we recovered a
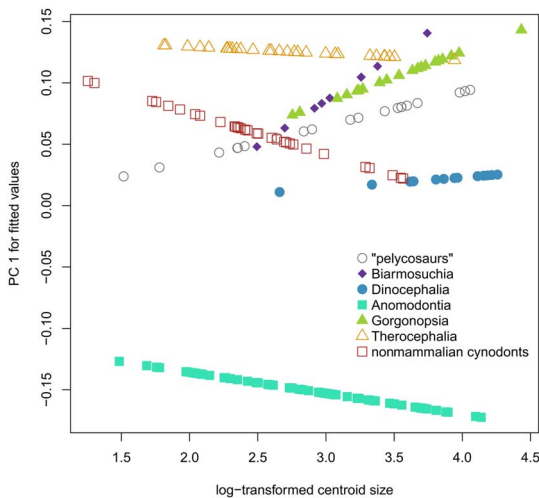

FIGURE 2.   Comparison of synapsid allometric trajectories. Log centroid size vs. predicted PC 1 scores of phylogenetic generalized least-squares regression of all shape components on log centroid size across 194 species of synapsids, organized by the seven main groups used for this study.

CREA-like pattern in the group, even when phylogenetic covariance was accounted for.

In "pelycosaurs," PC 3 correlates strongly with size (9.47% of variance; $R^2 = 0.293$, $p = 0.047$). High PC 3 loadings represent shapes with wedge-shaped snouts, a posteriorly shifted postorbital bar and posterior maxillary margin, and a dorsally shifted landmark 11, which relates to a jaw joint in line with the tooth row. Low PC 3 loadings represent shapes with a more "blocky" snout, anteriorly shifted postorbital bar and posterior maxillary margin, and a somewhat more sinusoidal ventral margin of the cranium (Supplementary Figure S3). These extremes differentiate between varanopid-like and sphenacodontid-like shapes.

Biarmosuchia.—In Biarmosuchia, we did not recover a significant interspecific allometric pattern ($R^2 = 0.397$, $p = 0.115$) using PGLS (Fig. 3). However, we note that a low sample size in this group may affect our ability to recover allometric trends.

Dinocephalia.—Our analyses did not recover a significant relationship between size and shape within the Dinocephalia ($R^2 = 0.117$, $p = 0.178$).

Anomodontia.—We did not recover a significant shared allometric trajectory within anomodonts independent of phylogeny ($R^2 = 0.0252$, $p = 0.242$), though the relationship between size and shape is stronger and significant when phylogenetic covariance is ignored ($R^2 = 0.0928$, $p = 0.001$) (see "Discussion"). In this shape-change regime, there is a transition from a shallow snout with a relatively small ventral displacement of the canine at small size to a deep snout and highly ventrally displaced canine at large size. The relative length of the snout does not change.

There is a strong relationship between geologic age and size in anomodonts (adjusted $R^2 = 0.294$, $p < 0.001$) and between size and phylogeny (Wilks's lambda = 0.999).

TABLE 3. Multivariate allometry. All shape components regressed against log-transformed centroid size. Numbers reported in bold represent non–phylogenetically corrected generalized least-squares (GLS) regressions; p-values below 0.05 reported in italics. *For Anomodontia and Therocephalia, we report ordinary least-squares/phylogenetic generalized least-squares (PGLS) regression results for better comparison with our results from ontogenetic series.

	Naïve allometry/PGLS allometry					
Taxon	Sum of squares	Mean sum of squares	R squared	F-statistic	Z-statistic	p
Synapsida	0.01105	0.0110547	0.019734	3.8853	1.8948	*0.0341*
Pelycosaurs	0.008734	0.0087336	0.21275	4.8644	2.0007	*0.019*
Biarmosuchia	0.0044004	0.0044004	0.39683	4.6053	1.2726	0.115
Dinocephalia	0.005258	0.0052579	0.09428	1.4573	0.89772	0.205
Anomodontia*	**0.1457**/0.007122	**0.145699**/0.0071222	**0.092787**/0.0252	**6.7503**/1.7062	**3.7278**/0.70842	***0.001***/*0.242*
Gorgonopsia	0.003654	0.0036545	0.090218	1.785	2.0404	*0.013*
Therocephalia*	**0.02608**/0.0071144	**0.0260795**/0.0071144	**0.09411**/0.12947	**2.8048**/4.0156	**2.1529**/2.99	***0.013***/*0.001*
Cynodontia	0.002983	0.0029831	0.051102	1.6156	−0.37819	0.664
Diictodon	**0.0502**	**0.050205**	**0.10731**	**4.2074**	**3.1769**	***0.001***
Theriognathus	**0.00606**	**0.0060602**	**0.039891**	**0.9972**	**0.25616**	**0.414**

Diictodon feliceps.—The pattern of intraspecific allometry in the dicynodont anomodont *D. feliceps* closely resembles the overall allometric trend across anomodonts recovered using OLS (Fig. 4), though the orbit is slightly larger in *D. feliceps*, likely because of the juvenile age of the smallest specimens (in contrast to the small-sized adults in the anomodont-wide data set). Likewise, the morphology of anomodonts at larger sizes represents a more extreme version of the *D. feliceps* large-size morphology, suggesting that the evolution of large size in the clade was accompanied by a stereotyped change in shape. *Diictodon* and anomodont allometric patterns have very similar trajectories, differing by 43.4° in 24-dimensional morphospace ($p = 0.0045$). The homogeneity of slopes test supports the null hypothesis that the anomodont and *D. feliceps* allometric trajectories are parallel ($p = 0.179$), further emphasizing the similar intraspecific and interspecific trends in the clade.

Gorgonopsia.—Using PGLS, we recovered a CREA-like pattern of shape change in Gorgonopsia ($R^2 = 0.0902$, $p = 0.013$) in which larger species have longer and deeper snouts than smaller species. Size also has a significant effect on PC 2 of shape variation in Gorgonopsia (PC 2 representing 20.27% of total shape variance; $R^2 = 0.175$, $p = 0.028$) (Supplementary Table S3), in which the overall pattern of shape change appears very similar to that recovered for overall size.

Therocephalia.—Contrary to the predictions of CREA, the snouts of small therocephalians tend to be slightly longer than the snouts of their larger relatives, though size explains a very small proportion of shape diversity ($R^2 = 0.0071$, $p = 0.001$) (Fig. 3). Size is correlated with the first two PC axes of shape variation in Therocephalia. The PC 1 of therocephalian morphospace (37.20% of variance; $R^2 = 0.0022$, $p = 0.02$) captures both the relative length and depth of the snout and the relative size of the orbit. At low PC 1 loadings, shapes have long, shallow snouts and large orbits, whereas at high PC 1 loadings, shapes have shorter, deeper snouts and small orbits. PC 2 of therocephalian morphospace (15.35% of variance; $R^2 = 0.0019$, $p = 0.011$) also significantly correlates with size: small shapes are deeper overall, whereas large shapes are shallow (Supplementary Fig. S2). This may correspond partially to taphonomic distortion, however. The crania of larger therocephalians have a much flatter dorsal profile than seen in smaller species. Some crania of large therocephalians in our data set appear to have been crushed dorsoventrally, with the skull roof being displaced ventrally, resulting in a very shallow braincase region, which may contribute to this pattern.

Theriognathus microps.—Ontogenetic patterns in *T. microps* do not follow those seen in Therocephalia as a whole (Fig. 5). Whereas Therocephalia exhibits distinct allometric trends, we did not recover any significant allometric trend in *T. microps* ($R^2 = 0.0398$, $p = 0.416$), corroborating the results of Huttenlocker and Abdala's (2016) revision of the
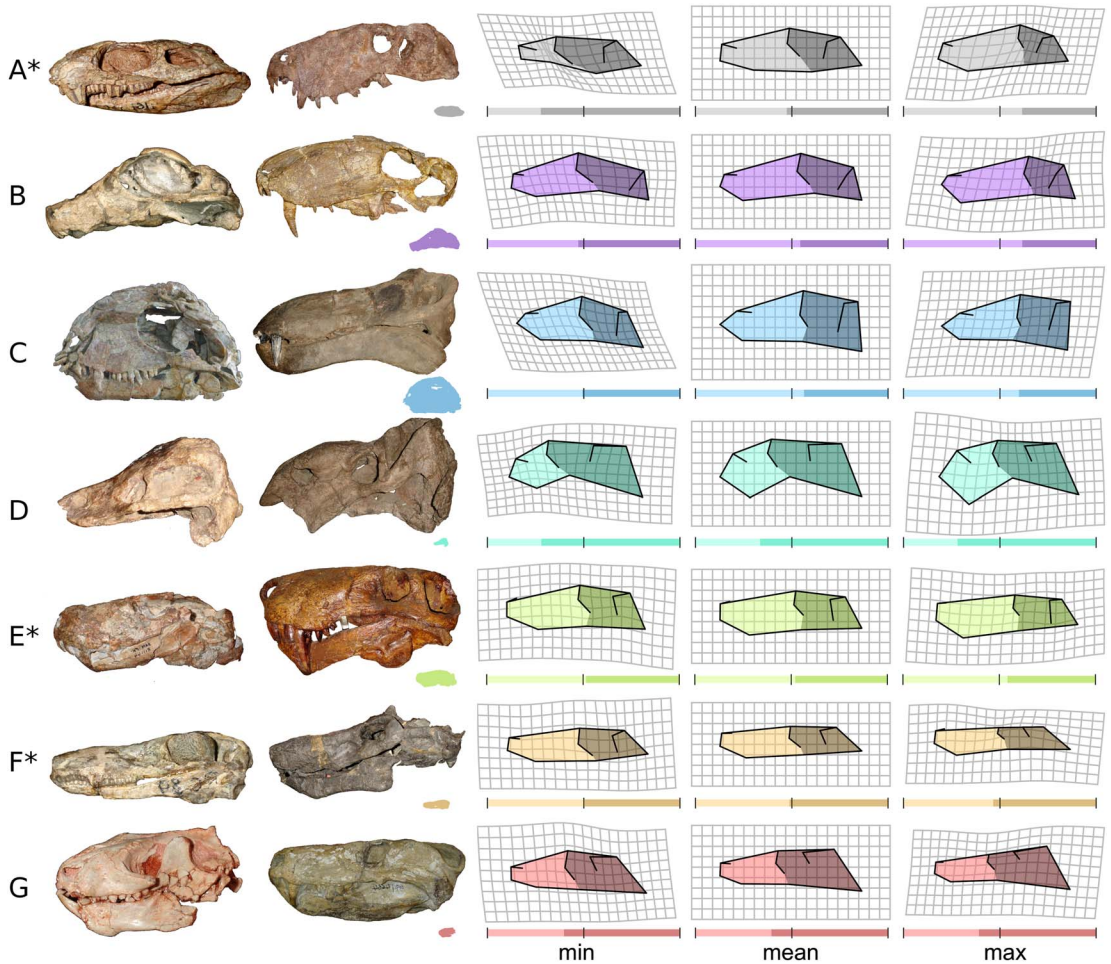
FIGURE 3. Representative specimens and predicted shapes. The first two columns display representative specimens from the largest and smallest ends of the size distribution in their groups to illustrate shape disparity in the crania. Specimens are not shown to scale, but the silhouettes of small specimens from the first column appear appropriately scaled next to large specimens from the second column to illustrate the magnitude of size differences in the group. The last three columns represent predicted minimum, mean, and maximum recovered shapes through a generalized least-squares (GLS) regression of all shape components on log-transformed centroid size. Shaded bars beneath the shapes illustrate the relative lengths of the snout and braincase regions, measured as the horizontal distance between landmarks 1 and 6 for the snout and landmarks 6 and 11 for the braincase. Only groups marked by an asterisk (*) show significant allometric trends when phylogeny is taken into account (see Table 3). Smallest and largest species are as follows: A, "pelycosaurs": *Eothyris parkeyi, Dimetrodon grandis*; B, Biarmosuchia: *Ictidorhinus martinsi, Biarmosuchus tener*; C, Dinocephalia: *Sinophoneus yumenensis, Jonkeria truculenta*; D, Anomodontia: *Kawingasaurus fossilis, Ischigualastia jenseni*; E, Gorgonopsia: *Eriphostoma microdon, Inostrancevia alexandri*; F, Therocephalia: *Tetracynodon darti, Scylacosaurus slateri*; G, Cynodontia: *Riograndia guaibensis, Cynognathus crateronotus*.

species. A homogeneity of slopes test comparing the allometric slopes of *T. microps* and Therocephalia as a whole rejected the null hypothesis of parallel slopes ($p = 0.02$). The angle between recovered allometric trajectories of *T. microps* and Therocephalia was not smaller than expected by chance (59.6°; $p = 0.066$).

Nonmammalian Cynodonts.—The relative contributions of snout and postorbital region to overall skull length do not change across the size range of nonmammalian cynodont, nor is there any overarching allometric pattern in nonmammalian cynodonts ($R^2 = 0.0511$, $p = 0.664$). Size does not significantly correlate with PC 1–3 of cynodont morphospace.
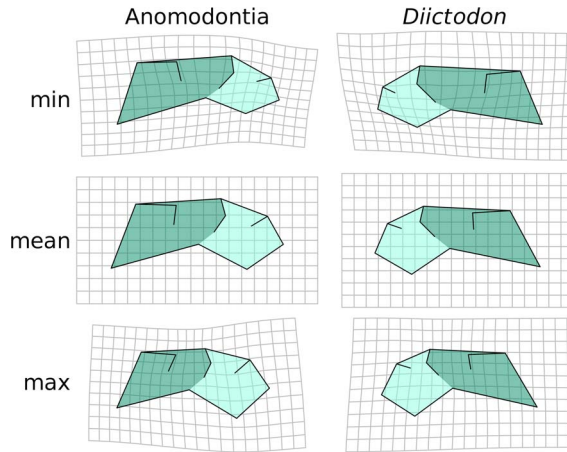
FIGURE 4.   *Diictodon* vs. anomodont allometry. Predicted shapes at minimum, mean, and maximum size of *Diictodon* and Anomodontia by a regression of all shape components on log-transformed centroid size. We present shapes shown in a mirrored configuration to highlight similarity through symmetrical arrangement.

Discussion

The central prediction of CREA is that larger animals will have proportionally longer snouts, a pattern based on relative lengths that could be recovered using three-dimensional, two-dimensional, or simple linear morphometrics. Though imperfect preservation and minor variations in photographic parameters likely have some effect on our results, we recovered many strong and significant signals that relate to both CREA and other patterns of synapsid allometry.

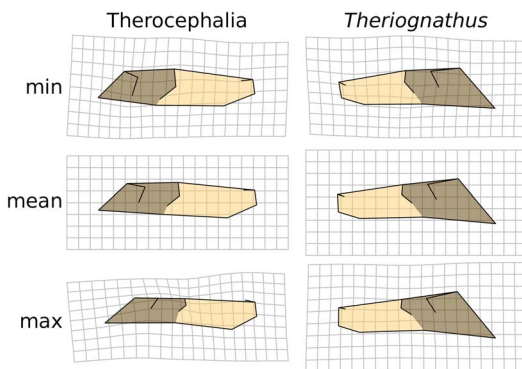There appears to be no universal pattern of interspecific allometry within nonmammalian

FIGURE 5.   *Theriognathus* vs. therocephalian allometry. Predicted shapes at minimum, mean, and maximum size of *Theriognathus* and Therocephalia by a regression of all shape components on log-transformed centroid size. We present shapes in a mirrored configuration to highlight similarity through symmetrical arrangement.

synapsid lineages (Fig. 2), though there are common traits. The relative contributions of snout and braincase to the total length of the skull account for a large amount of total variance within each group and within synapsids as a whole, as revealed by principal component analysis (Supplementary Table S4). However, this aspect of shape variation rarely correlates with size when phylogeny is taken into account. The only common features that seem to correlate with size across synapsids are a decrease in the relative size of the orbit in larger animals, a trend consistent with known allometric patterns across tetrapods (Howland et al. 2004), and an increased ventral displacement of the canine (landmark 4) (Fig. 3). Of the seven synapsid groups investigated, only two display a CREA-like pattern: "pelycosaurs" and Gorgonopsia.

In "pelycosaurs," we find support for Cardini and Polly's (2013) suggestion that variation in snout length is a key aspect of morphological disparity among skulls. PC 1, incorporating changes in snout length, accounts for 61.23% of variance, corroborating Goulds's (1967) finding that such variation was a major component of the "pelycosaur" radiation. Gould (1967) also proposed that snout length was strongly correlated with ecology in "pelycosaurs," with shorter snouts typifying herbivorous taxa. This relationship is common in many extant sauropsids (Claude

et al. 2004; Metzger and Herrel 2005; Stayton 2006) and seems related to the fact that a relatively short snout provides herbivorous taxa with a slow, powerful bite that is useful in processing plant material (Metzger and Herrel 2005). Therefore, the interconnected relationships between skull proportions and skull size in "pelycosaurs," and between diet and skull shape, might explain a distinctive aspect of the morphology of "pelycosaur" herbivores: their relatively small heads for their body sizes. Caseids, especially large members of the clade such as *Cotylorhynchus* (e.g., Stovall et al. 1966), are well known for their proportionally small skulls, and this phenomenon is also apparent, albeit to a lesser degree, in edaphosaurids. Conversely, faunivorous "pelycosaurs" are characterized by proportionally larger heads, a trend that is likely associated with lengthening the tooth row to accommodate a larger number of teeth and changing the mechanical advantage of the jaws to favor a fast, snapping bite (Gould 1967; Sakamoto 2010).

Unfortunately, our sample size for "pelycosaurs" is too small to allow detailed investigations of allometric patterns within the major subclades: despite an expansive postcranial record, complete, three-dimensionally preserved "pelycosaur" crania are rare. Further investigation and, ultimately, a larger number of complete cranial specimens will be needed to further test whether the apparent CREA-like pattern was indeed a ubiquitous feature of the grade (and possibly the ancestral character state for Synapsida), or an artifact of combining data from multiple clades that may have had distinct allometric relationships (and indeed may not all be closely related; see Ford and Benson 2018).

The Biarmosuchia represent a morphologically and presumably ecologically conservative group, despite their often elaborate cranial ornamentation, similar to the mammal clades investigated by Cardini and Polly (2013) and Cardini et al. (2015). Shape differences captured by PC 1 (explaining 47.50% of shape variance in the data set) (Supplementary Table S3) predominantly consist of relative lengthening of the snout, and this PC axis is strongly correlated with size. However, the relationship between size and shape is not independent of phylogeny. We therefore do not find support for a CREA-like allometric pattern in Biarmosuchia.

Likewise, we recovered no allometric pattern in Dinocephalia. This may be due to a combination of high disparity and the large average size of dinocephalians, which are ecologically and morphologically diverse but represented by very few species in our data set. Neither anteosaurs nor tapinocephalids appear to follow a CREA-like pattern, though low species diversity in both groups makes analysis difficult.

We recovered the strongest support for a CREA-like pattern in Gorgonopsia (Table 2). In this clade, the pattern of snout lengthening is subtle but significant, much like the pattern seen in mammalian clades (Cardini and Polly 2013; Cardini et al. 2015). Gorgonopsia is a morphologically conservative group (Kammerer and Masyutin 2018), and our sample of gorgonopsian crania had very low total shape variance compared with all other synapsid groups (Supplementary Fig. S3). Gorgonopsia are temporally constrained as well; only one species in our sample, *Eriphostoma microdon*, occurs outside the Lopingian. Because of their narrow temporal range and limited morphological variation, gorgonopsians may be the group in our study most comparable to those studied by Cardini and Polly (2013) and Cardini et al. (2015).

In therocephalians, the pattern of snout length is reversed, with the smallest therocephalians having the proportionally longest snouts and larger therocephalians having shorter snouts. Our investigation of ontogenetic shape change in the whaitsiid therocephalian *T. microps*, however, did not align with this clade-wide trend. Instead, we recovered largely isometric growth within this species, indicating a disconnect between ontogenetic and interspecific patterns of allometry. The lack of postcanine dentition in *Theriognathus* may obviate one of the main benefits of a longer snout, a longer tooth row, a result in line with Cardini and Polly's (2013) suggestion that CREA is linked to feeding efficiency.

Though "pelycosaurs" and gorgonopsians may follow a CREA-like pattern, the immediate

outgroups to mammals—nonmammalian cynodonts and therocephalians—show no adherence to CREA. There is no relationship between snout length and log centroid size in nonmammalian cynodonts, the closest relatives of crown Mammalia in our data set. This result parallels Hoffman and Rowe's (2018) recent discovery that relative snout length does not increase over ontogeny in the tritylodontid cynodont *Kayentatherium wellesi*. Taken together, these findings provide strong evidence for the specific CREA pattern observed in mammals having first appeared within Mammaliaformes rather than within nonmammalian synapsids, even if a similar allometric relationship was the basal character state for Synapsida and/or evolved independently in Gorgonopsia.

Our naïve regressions found strong support for a parallel relationship between ontogenetic allometry in *D. feliceps* and interspecific allometry of anomodonts (Fig. 4). However, the phylogenetically corrected regression results do not support a significant relationship between size and shape in Anomodontia. We believe that this finding may be related to both the specific evolutionary history of anomodonts and the properties of the PGLS regression. The anomodont tree used in our study is largely pectinate (Supplementary Fig. S1), with the most deeply nested clades containing the most geologically recent dicynodonts, many of which also are among the largest anomodonts. Though some earlier-diverging dicynodonts have very large skulls (e.g., *Endothiodon*, *Odontocyclops*, *Rhachiocephalus*), there is an extremely high degree of phylogenetic signal in centroid size in our data, as well as a strong trend of increasing size throughout anomodont history (Angielczyk and Walsh 2008; Griffin and Angielczyk 2019). This pattern of size evolution is certainly not independent of evolutionary history, and it results in phylogeny explaining the majority of anomodont shape variance when it is included as a term in the regression. Furthermore, if heterochronic development does indeed provide an evolutionary "path of least resistance" for changes in body size, we might expect there to be a large amount of phylogenetic signal in interspecific allometry associated with this path. Because of this combination of factors, we are reluctant to completely dismiss the significant size–shape relationship detected by our naïve regression, despite the contradictory results of PGLS regression.

If we accept the allometric pattern seen in the naïve regression across anomodonts, the close relationship to the ontogenetic pattern of *Diictodon* suggests an evolutionary link between ontogeny and size evolution in the clade. Anomodont size diversification likely occurred in part through a co-option of the ontogenetic process, with lineages changing size through heterochronic adjustments of a common ontogenetic plan. A probable example of this process can be found in changes in size in the dicynodont *Lystrosaurus* across the Permo-Triassic boundary documented by Botha-Brink et al. (2016). Late Permian *Lystrosaurus* in the Karoo Basin of South Africa, especially *L. maccaigi*, were relatively large dicynodonts with prolonged, multiyear growth and life spans of over a decade. In contrast, the Early Triassic species *L. declivis* and *L. murrayi* typically were smaller and had much shorter life spans (individuals over 2 years old at the time of death appear to be extremely rare). Although these changes in size and life history likely represent an adaptation to harsh and unpredictable conditions in the aftermath of the Permo-Triassic extinction (Botha-Brink et al. 2016), the mechanism by which the reduction in size occurred (progenesis sensu Alberch et al. 1980) is consistent with our hypothesis that heterochronic shifts were a viable means of size evolution in anomodonts.

The influence of shared ontogeny on interspecific allometry may explain not only the pattern in anomodonts, but in mammals as well. As noted earlier, Cardini et al. (2015) posited that the observed CREA pattern has a basis in ontogeny. If mammals follow stereotyped ontogenetic patterns, size evolution in the group may follow an ontogenetic axis; growth is arrested or prolonged to reach an advantageous adult body size. In this view, the CREA pattern, nearly ubiquitous in mammals (Fig. 6), is produced by size diversification co-opting a common ontogeny, and this may explain the lack of support for CREA in nonmammalian clades, which do not necessarily
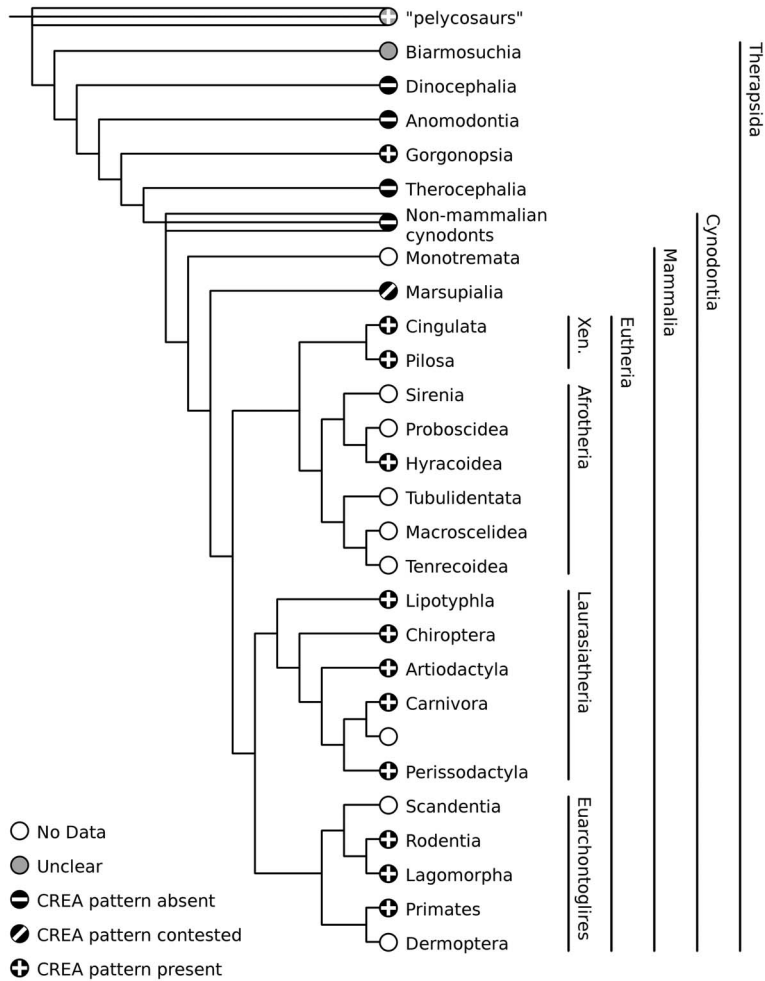
FIGURE 6. Prevalence of the CREA pattern in synapsids. Circle fill indicates whether the CREA pattern has been identified in that group or within a subclade of that group. Examples of the CREA pattern in mammals follow Cardini and Polly (2013) and Cardini (2019). Though the CREA pattern has been reported in Macropodids (Cardini et al. 2015), it appears to be driven by ecological adaptation (Mitchell et al. 2018) and therefore may not be a true example of evolutionary allometry. Because "pelycosaurs" represent a morphologically and ecologically disparate grade, the group as a whole does not correspond to the analyses confirming CREA in other groups and is therefore marked as present/unclear.

share mammalian ontogenetic patterns (e.g., Hoffman and Rowe 2018; this study).

If this explanation of CREA and anomodont allometry is correct, future investigations of ontogenetic pattern in nonmammalian synapsid clades such as biarmosuchians and gorgonopsians may reveal parallels between intraspecific ontogenetic allometry and interspecific allometry, even if a CREA-like pattern is not apparent. Moreover, it should be possible to detect similar parallelism between ontogeny and interspecific allometry in other clades, including the mammalian lineages originally investigated by Cardini and Polly (2013), Cardini et al. (2015), Tamagnini et al. (2017), and Cardini (2019). Cardini and Polly's "cranial rule" may not strictly describe the relationship between relative proportions of the snout and braincase, but may instead capture a more universally applicable pattern linking ontogenetic shape change to interspecific allometry.

Acknowledgments

Literature Cited

Adams, D. C., and Nistri, A. 2010. Ontogenetic convergence and evolution of foot morphology in European cave salamanders (Family: Plethodontidae). BMC Evolutionary Biology 10:1–10.

Adams, D. C., M. Collyer, A. Kaliontzopoulou, and E. Sherratt. 2016. Geomorph: software for geometric morphometric analyses. https://cran.r-project.org/web/packages/geomorph/index.html, accessed September 1, 2017.

Alberch, P., S. J. Gould, G. F. Oster, and D. B. Wake. 1980. Size and shape in ontogeny and phylogeny. Paleobiology 5:296–317.

Angielczyk, K. D., and C. F. Kammerer. 2017. The cranial morphology, phylogenetic position and biogeography of the Upper Permian dicynodont *Compsodon helmoedi* van Hoepen (Therapsida, Anomodontia). Papers in Palaeontology 3:513–545.

Angielczyk, K. D., and C. F. Kammerer. 2018. Non-mammalian synapsids: the deep roots of the mammalian family tree. Pp. 117–198 *in* F. E. Zachos and R. J. Asher, eds. Handbook of zoology: Mammalia: mammalian evolution, diversity and systematics. DeGruyter, Berlin.

Angielczyk, K. D., and M. Ruta. 2012. The roots of amphibian morphospace: a geometric morphometric analysis of Paleozoic temnospondyls. Fieldiana Life and Earth Sciences 5(October):40–58.

Angielczyk, K. D., and M. L. Walsh. 2008. Patterns in the evolution of nares size and secondary palate length in anomodont therapsids (Synapsida): implications for hypoxia as a cause of end-Permian tetrapod extinctions. Journal of Paleontology 82:528–542

Bell, M. A., and G. T. Lloyd. 2015. strap: an R package for plotting phylogenies against stratigraphy and assessing their stratigraphic congruence. Paleontology 58:379–389.

Benoit, J., F. Abdala, P. R. Manger, and B. S. Rubidge. 2016. The sixth sense in mammalian forerunners: variability of the parietal foramen and the evolution of the pineal eye in South African Permo-Triassic eutheriodont therapsids. Acta Palaeontologica Polonica 61:777–789.

Benton, M. J., P. C. J. Donoghue, R. J. Asher, M. Friedman, T. J. Near, and J. Vinther. 2015. Constraints on the timescale of animal evolutionary history. Palaeontologia Electronica 18.1.1FC:1–106.

Bhullar, B-A. S., J. Marugán-Lobón, F. Racimo, G. S. Bever, T. B. Rowe, M. A. Norell, and A. Abzhanov. 2012. Birds have paedomorphic dinosaur skulls. Nature 487:223–226.

Bookstein, F. L. 1991. Morphometric tools for landmark analysis: geometry and biology. Cambridge University Press, New York.

Botha-Brink, J., D. Codron., A. K. Huttenlocker, K. D. Angielczyk., and M. Ruta. 2016. Breeding young as a survival strategy during Earth's greatest mass extinction. Scientific Reports 6:24053.

Bright, J. A., J. Marugán-Lobón, S. N. Cobb, and E. J. Rayfield. 2016. The shapes of bird beaks are highly controlled by nondietary factors. Proceedings of the National Academy of Sciences USA 113:5352–5357.

Brocklehurst, N., R. R. Reisz, V. Fernandez, and J. Fröbisch. 2016. A re-description of *"Mycterosaurus" smithae*, an Early Permian eothyridid, and its impact on the phylogeny of pelycosaurian-grade synapsids. PLoS ONE 11:e0156810.

Brusatte, S. L., M. J. Benton, M. Ruta, and G. T. Lloyd. 2008. Superiority, competition, and opportunism in the evolutionary radiation of dinosaurs. Science 321:1485–1488.

Brusatte, S. L., M. Sakamoto, S. Montanari, and W. E. H. Harcourt Smith. 2012. The evolution of cranial form and function in theropod dinosaurs: insights from geometric morphometrics: geometric morphometrics of theropod dinosaurs. Journal of Evolutionary Biology 25:365–377.

Cardini, A. 2019. Craniofacial allometry is a rule in evolutionary radiations of placentals. Evolutionary Biology 46:239–248

Cardini, A., and P. D. Polly. 2013. Larger mammals have longer faces because of size-related constraints on skull form. Nature Communications 4:2458.

Cardini, A., P. D. Polly, R. Dawson, and N. Milne. 2015. Why the long face? Kangaroos and wallabies follow the same "rule" of cranial evolutionary allometry (CREA) as placentals. Evolutionary Biology 42:169–176.

Churchill, M., J. H. Geisler, B. L. Beatty, and A. Goswami. 2018. Evolution of cranial telescoping in echolocating whales (Cetacea: Odontoceti). Evolution 72:1092–1108.

Claude, J., P. C. H. Pritchard, H. Tong, E. Paradis, and J.-C. Auffray. 2004. Ecological correlates and evolutionary divergence in the skull of turtles: a geometric morphometric assessment. Systematic Biology 53:933–948.

Emerson, S. B., and D. M. Bramble. 1993. Scaling, allometry, and skull design. Pp. 384–421 *in* J. Hanken and B. K. Hall, eds. The skull 3. University of Chicago Press, Chicago.

Esteve-Altava, B., J. Marugán-Lobón, H. Botella, and D. Rasskin-Gutman. 2013. Structural constraints in the evolution of the tetrapod skull complexity: Williston's law revisited using network models. Evolutionary Biology 40:209–219.

Ford, D. P., and R. B. J. Benson. 2018. A redescription of *Orovenator mayorum* (Sauropsida, Diapsida) using high-resolution μCT, and the consequences for early amniote phylogeny. Papers in Palaeontology 5:197–239.

Foth, C., and O. W. M. Rauhut. 2013. Macroevolutionary and morphofunctional patterns in theropod skulls: a morphometric approach. Acta Palaeontologica Polonica 58:1–16.

Goswami, A. 2006. Cranial modularity shifts during mammalian evolution. American Naturalist 168:270–280.

Goswami, A., and P. D. Polly. 2010. The influence of modularity on cranial morphological disparity in Carnivora and primates (Mammalia). PLoS ONE 5:e9517.

Gould, S. J. 1967. Evolutionary patterns in pelycosaurian reptiles: a factor-analytic study. Evolution 21:385–401.

Gunz, P., P. Mitteroecker, S. Neubauer, G. W. Weber, and F. L. Bookstein. 2009. Principles for the virtual reconstruction of hominin crania. Journal of Human Evolution 57:48–62.

Griffin, C. T., and K. D. Angielczyk. 2019. The evolution of the dicynodont sacrum: constraint and innovation in the synapsid axial column. Paleobiology 45:201–220.

Hoffman, E. A., and T. B. Rowe. 2018. Jurassic stem-mammal perinates and the origin of mammalian reproduction and growth. Nature 561:104–108.

Hopson, J. A. 1991. Systematics of the nonmammalian Synapsida and implications for patterns of evolution in synapsids. Pp. 635–693 *in* H.-P. Schultze and L. Trueb, eds. Origins of the higher groups of tetrapods: controversy and consensus. Cornell University Press, Ithaca, N.Y.

Howland, H. C., S. Merola, and J. R. Basarab. 2004. The allometry and scaling of the size of vertebrate eyes. Vision Research 44:2043–2065.

Huttenlocker, A. K., and F. Abdala. 2016. Revision of the first therocephalian, *Theriognathus* Owen (Therapsida: Whaitsiidae), and implications for cranial ontogeny and allometry in nonmammaliaform eutheriodonts. Journal of Paleontology 89:645–664.

Kammerer, C. F. 2011. Systematics of the Anteosauria (Therapsida: Dinocephalia). Journal of Systematic Palaeontology 9:261–304.

Kammerer, C. F., and V. Masyutin. 2018. Gorgonopsian therapsids (*Nochnitsa* gen. nov. and *Viatkogorgon*) from the Permian Kotelnich locality of Russia. PeerJ 6:e4954.

Kemp, T. S. 1982. Mammal-like reptiles and the origin of mammals. Academic Press, New York.

Kemp, T. S. 2005. The origin and evolution of mammals. Oxford University Press, Oxford.

Kruger, A., B. S. Rubidge, F. Abdala, E. G. Chindebvu, and L. L. Jacobs. 2015. *Lende chiweta*, a new therapsid from Malawi, and its influence on burnetiamorph phylogeny and biogeography. Journal of Vertebrate Paleontology 35:e1008698.

Linde-Medina, M. 2016. Testing the cranial evolutionary allometric "rule" in Galliformes. Journal of Evolutionary Biology 29:1873–1878.

Martin, R. D., M. Genoud, and C.K. Hemelrijk. 2005. Problems of allometric scaling analysis: examples from mammalian reproductive biology. Journal of Experimental Biology 208: 1731–1747.

Metzger, K. A., and A. Herrel. 2005. Correlations between lizard cranial shape and diet: a quantitative, phylogenetically informed analysis. Biological Journal of the Linnean Society 86:433–466.

Mitchell, D. R., E. Sherratt, J. A. Ledogar, and S. Wroe. 2018. The biomechanics of foraging determines face length among kangaroos and their relatives. Proceedings of the Royal Society of London B 285:20180845.

R Core Team. 2017. A language and environment for statistical computing. R Foundation for Statistical Computing, Vienna, Austria. https://www.R-project.org, accessed September 1, 2017.

Radinsky, L. B. (1985) Approaches in evolutionary morphology: a search for patterns. Annual Review of Ecology and Systematics 16:1–14.

Revell, L. J. (2012) phytools: an R package for phylogenetic comparative biology (and other things). Methods in Ecology and Evolution 3:217–223.

Rohlf, F. J. 2016. TpsDig, Version 2.26 (Tps_Digitize). https://life.bio.sunysb.edu/morph, accessed September 1, 2017.

Ruta, M., J. Botha-Brink, S. A. Mitchell, and M. J. Benton. 2013. The radiation of cynodonts and the ground plan of mammalian morphological diversity. Proceedings of the Royal Society of London B 28:20131865.

Sakamoto, M. 2010. Jaw biomechanics and the evolution of biting performance in theropod dinosaurs. Proceedings of the Royal Society of London B 277:3327–3333.

Sherratt, E., D. J. Gower, C. P. Klingenberg, and M. Wilkinson. 2014. Evolution of cranial shape in caecilians (Amphibia: Gymnophiona). Evolutionary Biology 41:528–545.

Sidor, C. A. 2001. Simplification as a trend in synapsid cranial evolution. Evolution 55:1419–1442.

Sidor, C. A., and J. A. Hopson. 1998. Ghost lineages and "mammalness": assessing the temporal pattern of character acquisition in the Synapsida. Paleobiology 24:54–73.

Sigurdsen, T., A. K. Huttenlocker, S. P. Modesto, T. B. Rowe, and R. Damiani. 2012. Reassessment of the morphology and paleobiology of the therocephalian *Tetracynodon darti* (Therapsida), and the phylogenetic relationships of Baurioidea. Journal of Vertebrate Paleontology 32:1113–1134.

Stayton, C. T. 2005. Morphological evolution of the lizard skull: a geometric morphometrics survey. Journal of Morphology 263:47–59.

Stayton, C. T. 2006. Testing hypotheses of convergence with multivariate data: morphological and functional convergence among herbivorous lizards. Evolution 60:824–841.

Stovall, J. W., L. I. Price, and A. S. Romer. 1966. The postcranial skeleton of the giant Permian pelycosaur *Cotylorhynchus romeri*. Bulletin of the Museum of Comparative Zoology 135(1). Harvard University, Cambridge, Mass.

Tamagnini, D., C. Meloro, and A. Cardini, 2017. Anyone with a long-face? Craniofacial evolutionary allometry (CREA) in a family of short-faced mammals, the Felidae. Evolutionary Biology 44:476–495.

Zelditch, M. L., H. D. Sheets, and W. L. Fink. 2003. The ontogenetic dynamics of shape disparity. Paleobiology 29:139–156.

Zelditch, M. L., Z. T. Calamari, and D. L. Swiderski. 2016. Disparate postnatal ontogenies do not add to the shape disparity of infants. Evolutionary Biology 43:188–207.